AIP | Review of Scientific Instruments

Broadband ultrasonic linear array using ternary PIN-PMN-PT single crystal

Wei Wang, Xiangyong Zhao, Siu Wing Or, Chung Ming Leung, Yaoyao Zhang et al.

Citation: Rev. Sci. Instrum. **83**, 095001 (2012); doi: 10.1063/1.4748522

View online: http://dx.doi.org/10.1063/1.4748522

View Table of Contents: http://rsi.aip.org/resource/1/RSINAK/v83/i9

Published by the American Institute of Physics.

Broadband ultrasonic linear array using ternary PIN-PMN-PT single crystal

Wei Wang,[1,2,3,a)] Xiangyong Zhao,[1] Siu Wing Or,[2] Chung Ming Leung,[2] Yaoyao Zhang,[1,3] Jie Jiao,[1,3] and Haosu Luo[1]
[1]*Key Laboratory of Inorganic Functional Material and Device, Shanghai Institute of Ceramics, Chinese Academy of Sciences, Shanghai 201800, China*
[2]*Department of Electrical Engineering, The Hong Kong Polytechnic University, Hung Hom, Kowloon, Hong Kong*
[3]*Graduate School of the Chinese Academy of Sciences, Beijing 100049, China*

(Received 19 June 2012; accepted 14 August 2012; published online 4 September 2012)

Ternary $Pb(In_{1/2}Nb_{1/2})O_3$-$Pb(Mg_{1/3}Nb_{2/3})O_3$-$PbTiO_3$ (PIN-PMN-PT) single crystal was investigated for potential application in ultrasonic linear array. Orientation and temperature dependences of height extensional electromechanical coupling coefficient k'_{33} for PIN-PMN-PT single crystal were studied. It was found that the [001] poled PIN-PMN-PT diced along the [100] direction would achieve a maximum k'_{33} (~87%) and the service temperature was up to 110 °C. Ultrasonic linear arrays using PIN-PMN-PT single crystal and PZT ceramic were fabricated and compared. The bandwidth at −6 dB, two-way insertion loss and pulse length of the PIN-PMN-PT array were 98.6%, −45.1 dB, and 0.28 μs, respectively, which were about 25% broader, 3.7dB higher, and 0.08 μs shorter than those of the PZT array. The experimental results agreed well with the theoretical simulation. These superior performances were attributable to the excellent piezoelectric properties of PIN-PMN-PT single crystal. © *2012 American Institute of Physics*. [http://dx.doi.org/10.1063/1.4748522]

I. INTRODUCTION

Broadband ultrasonic arrays are essential for harmonic imaging, which has been developed in order to obtain both high resolution and deep penetration simultaneously in modern medical ultrasonic imaging systems.[1] Obtaining wide bandwidth from small piezoelectric elements used in array transducers is particularly difficult. Traditionally, lead zirconate titanate (PZT) ceramics are the most popular piezoelectric materials used in the fabrication of ultrasonic transducers because of their high performance and ease of manufacturing.[2] However, transducers made of PZT ceramics typically exhibit a bandwidth (−6 dB) of 60% to 70%, which is not sufficient to meet the full requirement of harmonic imaging. In the past decade, relaxor-based ferroelectric single crystals $Pb(Mg_{1/3}Nb_{2/3})$-$PbTiO_3$ (PMN-PT) and $Pb(Zn_{1/3}Nb_{2/3})$-$PbTiO_3$ (PZN-PT) have attracted considerable attention because of their extremely high piezoelectric and electromechanical coupling coefficients near the morphotropic phase boundary (MPB) composition ($d_{33} \approx 2000$ pC/N, $k_{33} \approx 0.92$).[3–5] Researches on PMN-PT and PZN-PT single crystals have been carried out in the field of medical ultrasonic applications and some attractive results have been found.[6–9] Single crystal piezoelectrics have brought out a revolutionary development for ultrasonic transducers in modern medical ultrasonic imaging systems.

More recently, high Curie temperature (T_C) crystals have been developed in order to make the devices maintain better stability. Among the various series of piezoelectric materials, ternary single crystal $Pb(In_{1/2}Nb_{1/2})O_3$-$Pb(Mg_{1/3}Nb_{2/3})O_3$-$PbTiO_3$ (PIN-PMN-PT or PIMNT) has been considered as another promising candidate because of its high Curie temperature and excellent piezoelectric performance.[10–15] Although some works have been carried out on PIN-PMN-PT single-element ultrasonic transducers,[16,17] the linear and phased arrays using PIN-PMN-PT single crystal have not been reported. This paper does not only demonstrate the relevant piezoelectric properties of PIN-PMN-PT single crystal for array applications, but also the fabrication and characterization of a 3.0 MHz, 32-channel ultrasonic linear array using PIN-PMN-PT single crystal. Meanwhile, a PZT ceramic linear array with same center frequency was also fabricated for comparison.

II. EXPERIMENTAL PROCEDURE

A. Material preparation

PIN-PMN-PT single crystal with the composition of 0.35PIN-0.35PMN-0.30PT was grown directly from their melt by the modified Bridgman technique in our laboratory.[14,18] The boule size is Φ50 mm × 80 mm and the available plate size can reach 30 mm × 30 mm, as shown in Fig. 1. The as-grown crystal was oriented along the [001], [1$\bar{1}$0] and [010] directions using an x-ray diffractometer and then sliced into (001) wafers. Chromium-gold (Cr/Au) layers of thickness 50/100 nm were sputtered on the main surfaces as electrodes at 200 °C. Then, the crystals were poled under an electric field of 15 kV/cm in silicone oil for 15 min at 135 °C. Due to the anisotropy of crystallographic alignment, a group of height extensional resonators were investigated to determine the optimal crystal cut for [001] poled PIN-PMN-PT single crystal. Figure 2 shows the as-prepared resonators with length orientation varying from [1$\bar{1}$0] to [100] direction every 5°. According to the IEEE standards,[19] the height extensional coupling coefficient k'_{33} was calculated by the

a)Electronic mail: wwang1008@hotmail.com.

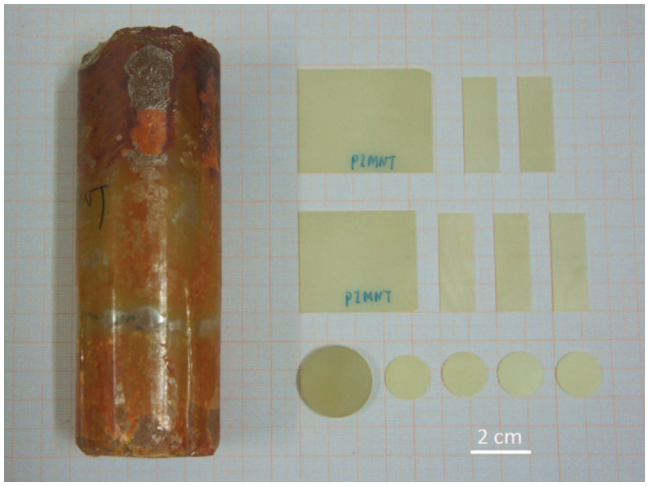

FIG. 1. PIN-PMN-PT single crystals grown by modified Bridgeman method. The boule size can reach Φ50 mm × 80 mm and the plate size can reach 30 mm × 30 mm.

following formulas:

$$k'_{33} = \sqrt{\frac{\pi}{2}\frac{f_r}{f_a}\tan\left(\frac{\pi}{2}\frac{f_a - f_r}{f_a}\right)}, \quad (1)$$

where f_r and f_a represent the resonance and anti-resonance frequencies determined by an HP4294A impedance analyzer, respectively. Besides, the samples were heated in OXFORD MicrostatN cryostat combining with ITC502 temperature controller to evaluate the thermal stability of PIN-PMN-PT crystal.

B. Design of the ultrasonic linear arrays

The piezoelectric elements with high piezoelectric and electromechanical performance would improve the sensitivity and bandwidth of the array. In this work, both PIN-PMN-PT single crystal and traditional PZT ceramic (PZT-5H) were chosen for array fabrication and comparison, the PZT ceramic was commercially supplied by PANT Piezoelectric Tech Co., LTD. The measured properties of the PIN-PMN-PT single crystal and PZT ceramic are summarized in Table I. Figure 3 shows the structure of the designed ultrasonic linear array (Fig. 3(a)) and dimensions of the PIN-PMN-PT array element (Fig. 3(b)). For medical ultrasonic application, human tissue with an acoustic impedance of ~1.5 MRayls was used to be load medium which is much smaller than that of PIN-PMN-PT single crystal (~26 MRayls). Hence, two matching layers were adopted for array fabrication. The

TABLE I. Measured material parameters of [001] poled PIN-PMN-PT single crystal and PZT ceramic used for array simulation and fabrication.

	PIN-PMN-PT	PZT(PZT-5H)
Electromechanical coupling coefficient k'_{33}	87%	69%
Piezoelectric charge coefficient d_{33} (pC/N)	1700	700
Free dielectric constant ε_{33}^{T}	4300	3500
Dissipation factor tan δ	0.007	0.015
Density ρ (kg/m^3)	8000	7500
Longitudinal acoustic velocity v'_{33} (m/s)	3240	3860
Acoustic impedance Z'_{33} (MRayl)	25.9	29.0

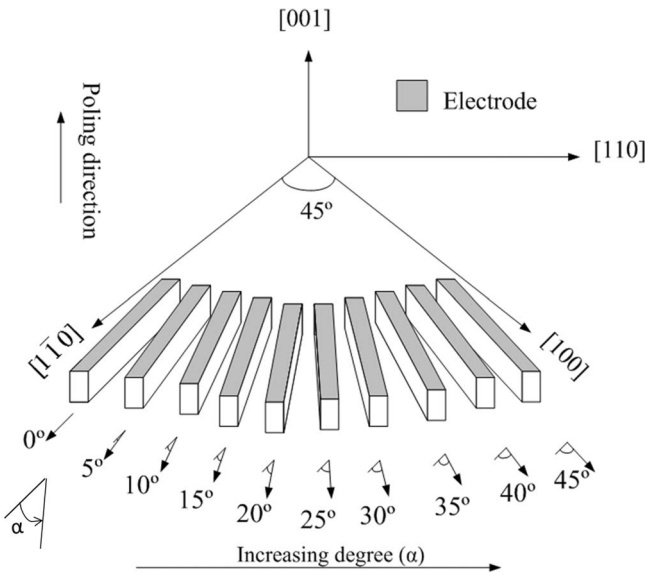

FIG. 2. The length orientation of height extensional PIN-PMN-PT resonators investigated.

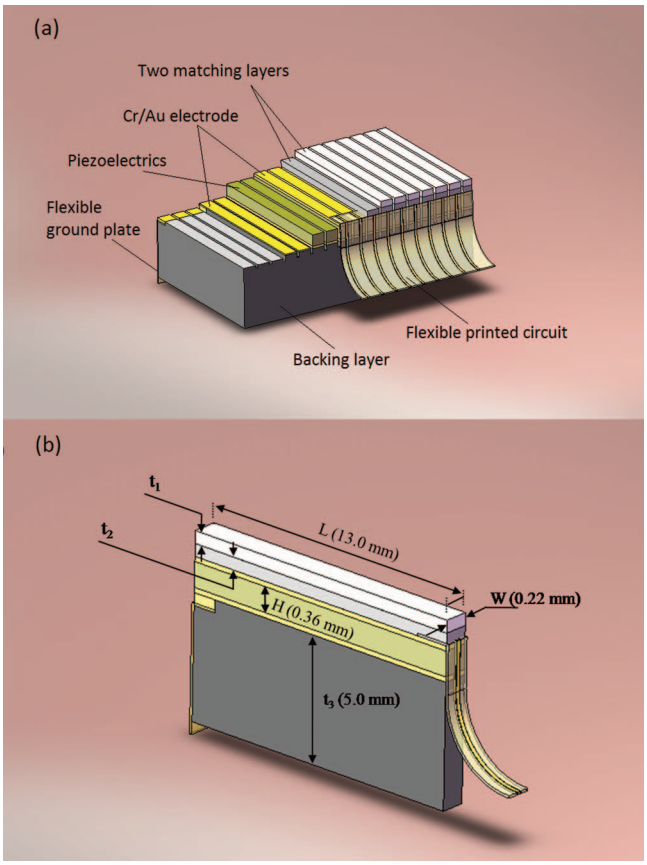

FIG. 3. (a) The structure of the designed ultrasonic linear array; (b) the dimensions of the PIN-PMN-PT array element.

TABLE II. The properties of the passive materials used for array simulation and fabrication.

Material	Use	v (m/s)	ρ (kg/m^3)	Z (MRayl)
Epo-Tek 301	Outer matching layer	2650	1150	3.1
Tungsten powder/Epo-Tek 301	Inner matching layer	1590	4800	7.6
Zirconia powder/Epo-Tek 301	Backing layer	2860	2800	8.0

optimal acoustic impedance Z_{m1} (inner), Z_{m2} (outer), and thickness t_1, t_2 of the matching layers could be determined by the following equations according to the KLM model:[20]

$$Z_{m1} = \left(Z_1^4 Z_2^3\right)^{1/7}, \tag{2}$$

$$Z_{m2} = \left(Z_1 Z_2^6\right)^{1/7}, \tag{3}$$

$$t_1 = \frac{\lambda_1}{4}, \tag{4}$$

$$t_2 = \frac{\lambda_2}{4}, \tag{5}$$

where Z_1 and Z_2 are the acoustic impedance of the piezoelectric material and load medium, respectively. λ_1 and λ_2 are the wavelength of the acoustic wave at center frequency in the inner and outer matching layers, respectively. According to the above equations, the calculated Z_{m1} and Z_{m2} were 7.7 and 2.3 MRayls, respectively. The acoustic impedance of backing layer was determined as 8.0 MRayls by the consideration of bandwidth and signal amplitude comprehensively. A PZT ceramic linear array was also designed by following the same rules. Base on the simulation and previous experiments, epoxy Epo-Tek 301 (Epoxy technology Inc., Billerica, MA) mixed with tungsten or zirconia powder were selected as the matching layer and backing layer materials. The properties of the passive materials used for the array simulation and fabrications are listed in Table II.

Before fabrication, the KLM equivalent circuit based software package PiezoCAD (Sonic Concepts, Woodinville, WA) was used for the evaluation of array design. The theoretical waveforms and frequency spectrum of the designed PIN-PMN-PT array and PZT array are shown in Fig. 4, respectively. The center frequency (f_c), relative bandwidth at −6 dB (BW), pulse length, and two-way insertion loss (IL) are summarized in Table III. Simulation results indicate that 20% broader bandwidth (−6 dB), 20% shorter pulse length, 4 dB higher sensitivity can be obtained compared to the PZT array.

C. Fabrication of ultrasonic arrays

The PIN-PMN-PT single-crystal array with a center frequency of 3.0 MHz, 32 elements, and each dimensions of 13 mm × 0.22 mm was fabricated in this report. The [001] poled PIN-PMN-PT wafer was prepared with the crystal cut

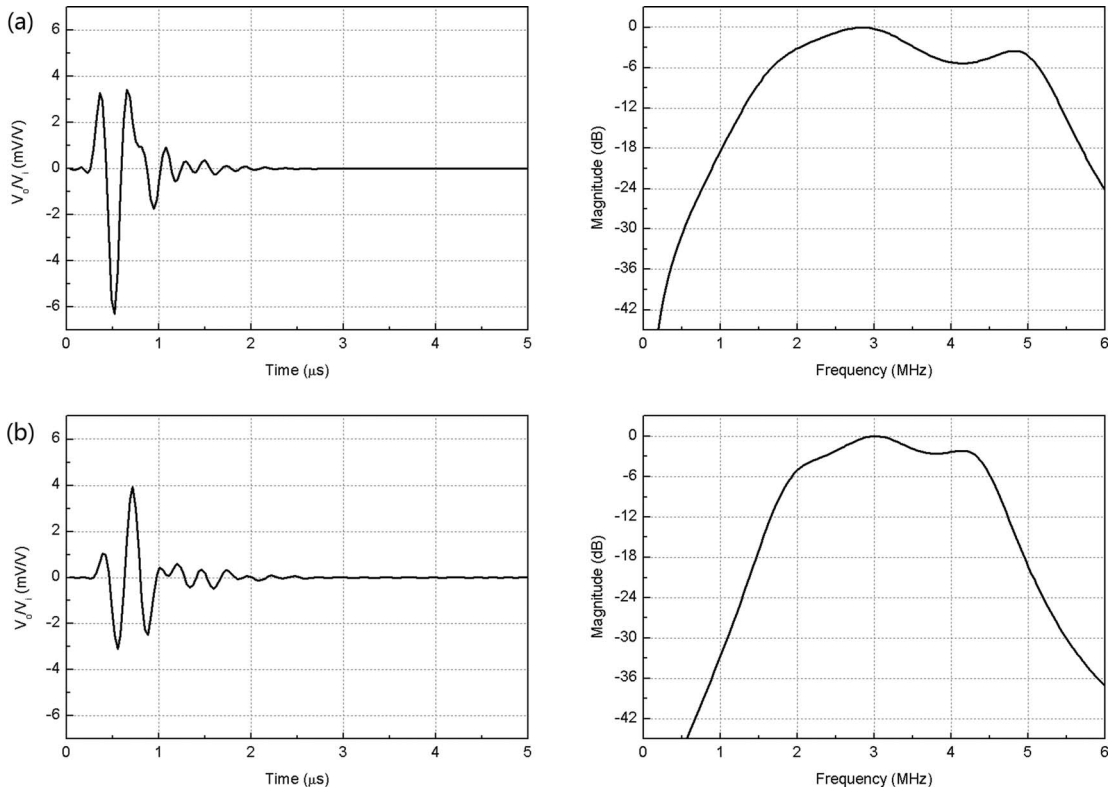

FIG. 4. The theoretical waveforms and frequency spectrums of the designed (a) PIN-PMN-PT array and (b) PZT array simulated using the PiezoCAD software.

TABLE III. Performances of the designed ultrasonic linear arrays using PIN-PMN-PT single crystal and PZT ceramic by the simulation.

	f_c (MHz)	BW @ −6 dB (%)	Pulse length (μs)	Pk Ampl (dB, re 1 V/V)
PIN-PMN-PT array	3.1	102.2%	0.323	−43.99
PZT array	3.0	80.3%	0.395	−48.12

and dimensions of $13[100]^L \times 10[010]^W \times 0.36[001]^T$ mm^3 (L: length, W: width, T: thickness). The outer and inner matching layers with thickness of 0.23 mm and 0.13 mm were cured at room temperature for 24 h. The fabricated matching layers were adhered to the upper surface of the prepared PIN-PMN-PT wafer using epoxy Epo-Tek 301, and external pressure equipment was employed here to provide a thin bonding layer (<0.5 μm). Then, a flexible printed circuit with 120 μm gold wire arranged with a constant pitch of 280 μm was bonded on the edge of the top electrode using an electrically conductive adhesive E-solder 3022 (Von Roll Isola USA Inc., Schenectady, NY) cured at room temperature for 24 h. The common ground wire with thickness of 0.5 mm was formed on the edge of the bottom electrode using E-solder 3022. After that, the backing layer with thickness of 5.0 mm was cured on the bottom electrode of the wafer. Finally, the dicing process was performed with a dicing saw (DISCO, Tokyo, Japan, Model DAD 321) using a 50-μm-thick nickel/diamond blade. The depth of dicing was set to 0.30 mm into the backing material, thus cutting through the matching layers and the piezoelectric material, while the bottom electrodes of all elements were electrically connected. The dicing pitch and measured kerf width were 0.28 mm and 0.06 mm, respectively. Hence the actual width of an array element was 0.28−0.06 = 0.22 mm. The width-to-height ratio of the array element was about 0.6, which was acceptable for PIN-PMN-PT single crystal to generate uncoupled resonance. The feeding speed was reduced to 0.4 mm/s, much slower than that of the PZT array. After dicing, acoustic kerfs were formed to eliminate the cross talk between neighbor elements. The PZT ceramic array was fabricated by following the same process as the PIN-PMN-PT array. The thickness of the PZT was about 0.58 mm, which was thicker than that of the PIN-PMN-PT because of the difference in the electromechanical coupling coefficient and frequency constant between the two piezoelectric materials.

III. RESULTS AND DISCUSSION

A. Properties of the PIN-PMN-PT single crystal

Figure 5 shows the calculated k'_{33} of the height extensional PIN-PMN-PT resonators with different length orientation. It was found that the k'_{33} increased gradually from 71% to 87% when the length orientation varies from $[1\bar{1}0]$ to [100] direction. Interesting, the [001] poled PIN-PMN-PT resonator diced along the [100] direction yielded an uncoupled resonance mode and achieved a maximum k'_{33} (= 87%), which was much superior to the PZT resonator (k'_{33} = 69%). Figure 6 shows the measured impedance and phase angle spectra for PIN-PMN-PT and PZT resonators in room temperature. With maintaining the same resonance frequency (f_r), the anti-resonance frequency (f_a) of PIN-PMN-PT resonator was larger than that of PZT ceramic. The larger impedance value at f_a and smaller impedance value at f_r of PIN-PMN-PT indicate a higher free dielectric constant and lower clamped dielectric constant of PIN-PMN-PT single crystal compared with PZT ceramic.

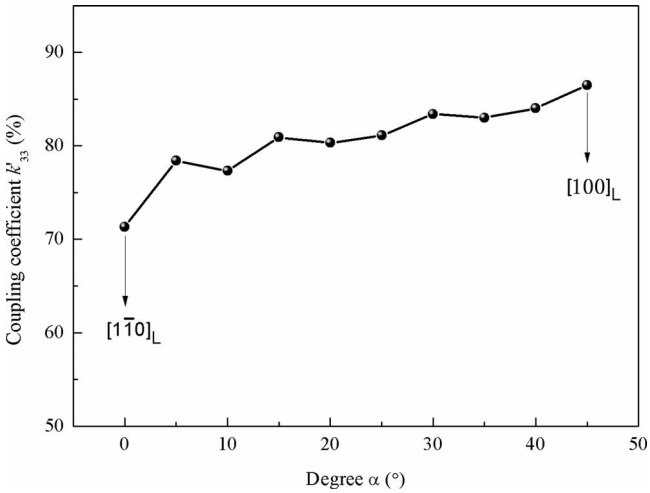

FIG. 5. The distribution of k'_{33} values in PIN-PMN-PT resonators with different length orientation.

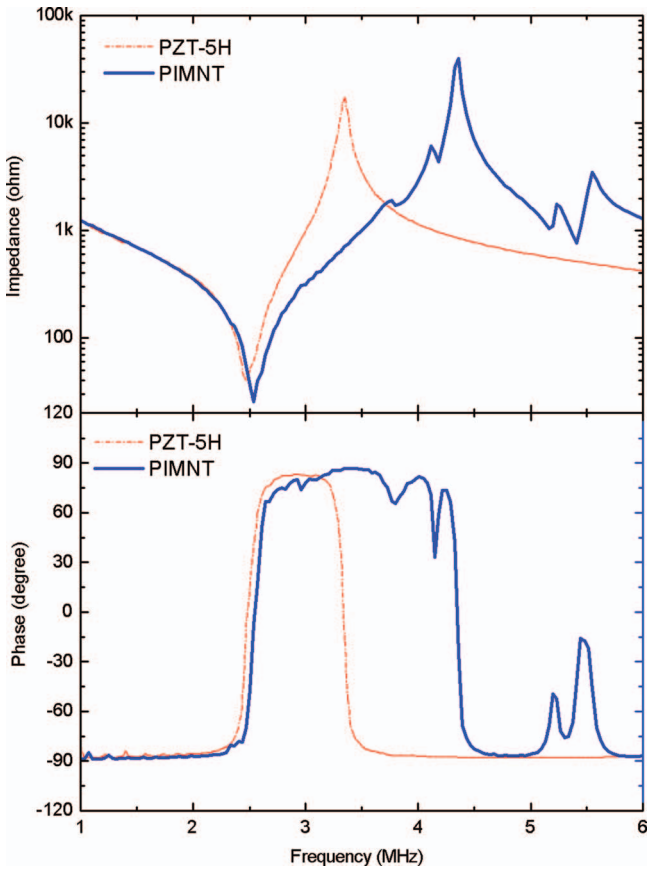

FIG. 6. The impedance and phase angle spectra for PIN-PMN-PT resonator and PZT resonator in room temperature.

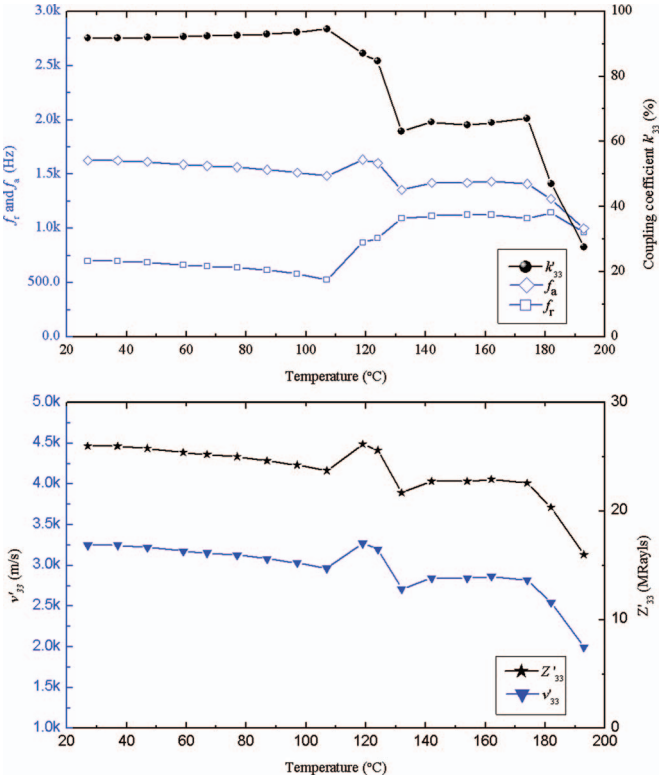

FIG. 7. (a) Temperature dependence of the resonant frequency (f_r), anti-resonant frequency (f_a) and the calculated k'_{33}; (b) the acoustic velocity (v'_{33}) and acoustic impedance (Z'_{33}) of PIN-PMN-PT single crystal.

Figure 7 shows the temperature-dependent f_r, f_a, calculated k'_{33}, v'_{33} (acoustic velocity), and Z'_{33} (acoustic impedance) of PIN-PMN-PT single crystal. Below 110 °C, around the rhombohedral to tetragonal phase transition temperature T_{rt} of PIN-PMN-PT single crystal, both f_r and f_a decreased slowly as the temperature increased and k'_{33} was nearly temperature independent. After that, both f_r and f_a increased suddenly. Since the increment of f_a was faster than that of f_r, according to Eq. (1), the corresponding k'_{33} decreased sharply to 65%. When the temperature increased to 180 °C, around the Curie temperature T_c of PIN-PMN-PT single crystal, f_r and f_a were close to each other. In the meanwhile, a further decrement of k'_{33} was found because of the depolarization phenomenon of PIN-PMN-PT single crystal at high temperature. The acoustic velocity v'_{33} and acoustic impedance Z'_{33}, shown in Fig. 6(b), followed a similar trend as found in the f_a.

B. Performance of the PIN-PMN-PT single-crystal linear array

The performances of the fabricated arrays were measured by using a conventional pulse-echo response measurement method.[21] The array was mounted on a holder and immersed in a water tank with a stainless steel target placed inside. By connecting to an ultrasonic pulser-receiver (Panametrics 5900PR, Olympus, Japan), the transducer was excited by a 1 μJ electrical impulse with 1 kHz reputation and

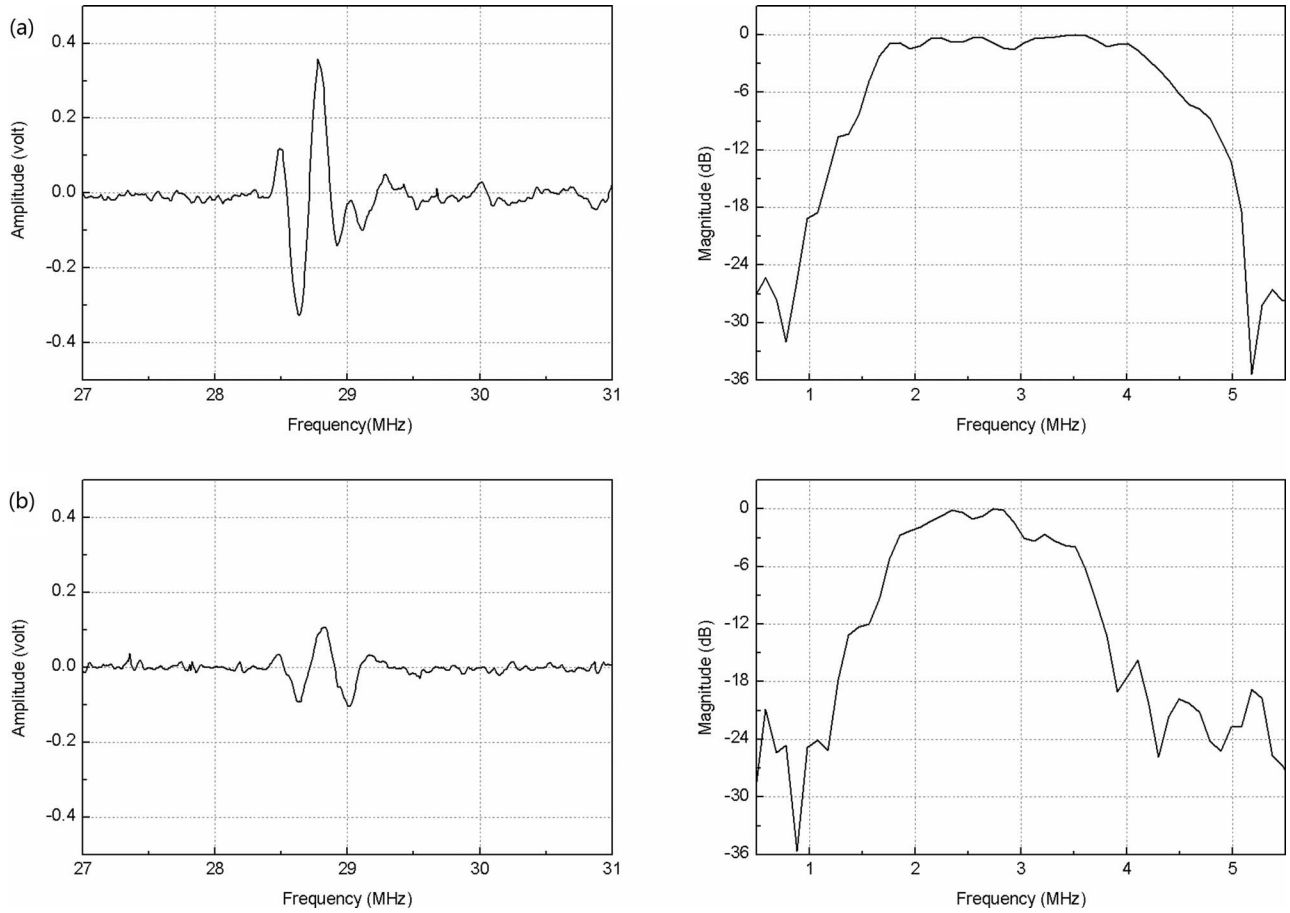

FIG. 8. The practical waveforms and frequency spectrums of the fabricated (a) PIN-PMN-PT array and (b) PZT array.

50 Ω damping factor. The echo response was captured and displayed on an oscilloscope (Infinium 54810A, HP, USA). The frequency spectrum of echo was obtained by applying FFT, using a function built-in to the oscilloscope. The center frequency (f_c) and −6 dB bandwidth (BW) of the transducer were determined from the measured frequency spectrum:

$$f_c = \frac{1}{2}(f_1 + f_2), \tag{6}$$

$$BW = \frac{f_2 - f_1}{f_C} \times 100\%, \tag{7}$$

where f_1 and f_2 are the lower and upper −6 dB frequencies, respectively.

The two-way insertion loss (IL) or the relative pulse-echo sensitivity is the ratio of the output power P_0 of the transducer to the input power P_i delivered to the transducer from the driving source. By assuming that the input load resistance R_i and output load resistance R_o are equal, the IL can be simplified as follows:

$$IL = 10\log\left(\frac{P_o}{P_i}\right) = 10\log\left(\frac{V_o^2/R_o}{V_i^2/R_i}\right) = 20\log\left(\frac{V_o}{V_i}\right), \tag{8}$$

The transducer was connected to a function generator (HP 8116A, USA), which was used to generate a tone burst of 20-cycle sine wave at f_c. The echo signal received by the transducer with V_o was measured by the oscilloscope with 1 MΩ coupling. The amplitude of the driving signal V_i was measured with 50 Ω coupling.

Figure 8 shows the practical waveforms and frequency spectrums of the fabricated (a) PIN-PMN-PT array and (b) PZT array. From Eqs. (6)–(8), the center frequency (f_c), relative bandwidth at −6 dB (BW) and two-way insertion loss (IL) were calculated and summarized in Table IV. The −6 dB bandwidth of the PIN-PMN-PT array can reach up to 98.6%, more than 25% broader than that of the PZT array. The bandwidth of the PIN-PMN-PT array, 1.52 to 4.49 MHz, included that of the PZT array, 1.74 to 3.59 MHz. This means that many reference frequencies can be selected for the PIN-PMN-PT array. Besides, the PIN-PMN-PT array exhibited a shorter impulse response (∼0.28 μs) than PZT array (∼0.36 μs), which can be expected to improve axial resolution. Additionally, the echo signal achieved by the PIN-PMN-PT array was about 3 dB larger than that of PZT array, indicating a higher sensitivity, which can be attributed to the larger d_{33} and k'_{33} of PIN-PMN-PT single crystal. The experimental results of the PIN-PMN-PT and PZT arrays agreed quite well with the predictions of simulation by PiezoCAD software.

TABLE IV. Performances of the fabricated ultrasonic linear arrays using PIN-PMN-PT single crystal and PZT ceramic.

	f_c (MHz)	BW @ −6 dB (%)	Pulse length (μs)	IL (dB)
PIN-PMN-PT array	3.0	98.6%	0.28	−45.1
PZT array	2.7	69.9%	0.36	−48.8

IV. CONCLUSION

To sum up, the height extensional electromechanical coupling coefficient k'_{33} for PIN-PMN-PT single crystal has been investigated systematically. The maximum k'_{33} as high as 87% can be achieved when the [001] poled PIN-PMN-PT diced along the [100] direction, and the service temperature is up to 110 °C. Two types of ultrasonic linear arrays using PIN-PMN-PT single crystal and PZT ceramic were fabricated and compared. The experimental results revealed that more than 25% broader bandwidth, 3.7 dB higher sensitivity, and 22% shorter pulse length can be obtained by using PIN-PMN-PT single crystal compared to the PZT array. The experimental results agreed very well with the theoretical simulation results. These indicate that the PIN-PMN-PT single crystal is a promising candidate in the revolution of medical ultrasonic linear and phased arrays with broad bandwidth, high sensitivity, and good resolution.

ACKNOWLEDGMENTS

This work was financially supported by the Ministry of Science and Technology of China through 973 Program (Grant No. 2009CB623305) and National Key Technology R&D Program (Grant No. 2010BAK69B26), the Natural Science Foundation of China (Grant Nos. 60837003, 61001041, and 11090332), Science and Technology Commission of Shanghai Municipality (Grant Nos. 10520712700, 10JC1415900, and 10dz0583400), the Innovation Fund of Shanghai Institute of Ceramics (Grant Nos. O99ZC4140G and O99ZC1110G), Shanghai Rising-Star Program (Grant No. 11QA1407500), Open Project from Shanghai Institute of Technical Physics, CAS (Grant No. IIMDKFJJ-11-08), and The Hong Kong Polytechnic University (I-ZV7P and G-U741).

[1] J. Chen and R. Panda, Proc.-IEEE Ultrason. Symp. **1-4**, 235 (2005).
[2] J. A. Gallego-Juarez, J. Phys. E: Sci. Instrum. **22**, 804 (1989).
[3] R. F. Service, Science **275**, 1878 (1997).
[4] S. E. Park and T. R. Shrout, J. Appl. Phys. **82**, 1804 (1997).
[5] Z. W. Yin, H. S. Luo, P. C. Wang, and G. S. Xu, Ferroelectrics **229**, 207 (1999).
[6] S. T. Lau, H. Li, K. S. Wong, Q. F. Zhou, D. Zhou, Y. C. Li, H. S. Luo, K. K. Shung, and J. Y. Dai, J. Appl. Phys. **105**, 094908 (2009).
[7] S. M. Rhim, H. Jung, S. Kim, and S. Lee, Proc.-IEEE Ultrason. Symp. **2**, 1143 (2002).
[8] S. Saitoh, T. Takeuchi, T. Kobayashi, K. Harada, S. Shimanuki, and Y. Yamashita, IEEE Trans. Ultrason. Ferroelectr. Freq. Control **46**, 414 (1999).
[9] C. G. Oakley, and M. J. Zipparo, Proc.-IEEE Ultrason. Symp. **2**, 1157 (2000).
[10] G. S. Xu, K. Chen, D. F. Yang, and J. B. Li, Appl. Phys. Lett. **90**, 032901 (2007).
[11] J. Tian, P. D. Han, X. L. Huang, H. X. Pan, J. F. Carroll, and D. A. Payne, Appl. Phys. Lett. **91**, 222903 (2007).
[12] D. A. Liu, Y. Y. Zhang, W. Wang, B. Ren, Q. Zhang, J. Jiao, X. Y. Zhao, and H. S. Luo, J. Alloys Compd. **506**, 428 (2010).
[13] S. J. Zhang, J. Luo, W. Hackenberger, and T. R. Shrout, J. Appl. Phys. **104**, 064106 (2008).
[14] Y. Y. Zhang, X. B. Li, D. Liu, Q. Zhang, W. Wang, B. Ren, D. Lin, X. Y. Zhao, and H. S. Luo, J. Cryst. Growth **318**, 890 (2011).

[15]W. Wang, D. Liu, Q. H. Zhang, B. Ren, Y. Y. Zhang, J. Jiao, D. Lin, X. Y. Zhao, and H. S. Luo, J. Appl. Phys. **107**, 084101 (2010).
[16]P. Sun, Q. Zhou, B. Zhu, D. Wu, C. Hu, J. M. Cannata, J. Tian, P. Han, G. Wang, and K. K. Shung, IEEE Trans. Ultrason. Ferroelectr. Freq. Control **56**, 2760 (2009).
[17]D. Zhou, K. F. Cheung, K. H. Lam, Y. Chen, Y. C. Chiu, J. Dai, and H. L. W. Chan, H. S. Luo, Rev. Sci. Instrum. **82**, 055110 (2011).
[18]H. S. Luo, G. S. Xu, H. Xu, P. C. Wang, and Z. W. Yin, Jpn. J. Appl. Phys. **39**, 5581 (2000).
[19]ANSI/IEEE Std. 176-1987, IEEE Standard on Piezoelectricity.
[20]C. S. Desilets, J. D. Fraser, and G. S. Kino, IEEE Trans. Sonics Ultrason. **SU-25(3)**, 115 (1978).
[21]K. R. Erikson, R. A. Banjavic, and P. L. Carson, J. Ultrasound Med. **1**, 1 (1982).